



POTSDAM-INSTITUT FÜR
KLIMAFOLGENFORSCHUNG

Originally published as:

[Wunderling, N.](#), [Winkelmann, R.](#), [Rockström, J.](#), [Loriani, S.](#), McKay, D. I. A., Ritchie, P. D. L., [Sakschewski, B.](#), [Donges, J. F.](#) (2023): Global warming overshoots increase risks of climate tipping cascades in a network model. - Nature Climate Change, 13, 75-82.

DOI: <https://doi.org/10.1038/s41558-022-01545-9>

Global warming overshoots increase risks of climate tipping cascades in a network model

Nico Wunderling,^{1,2,3*} Ricarda Winkelmann,^{1,4} Johan Rockström,^{1,2}
Sina Loriani,¹ David I. Armstrong McKay,^{2,5,6} Paul D.L. Ritchie,⁵
Boris Sakschewski,¹ and Jonathan F. Donges^{1,2,3*}

¹Potsdam Institute for Climate Impact Research (PIK), Member of the Leibniz Association,
14473 Potsdam, Germany

²Stockholm Resilience Centre, Stockholm University, Stockholm, SE-10691, Sweden

³High Meadows Environmental Institute, Princeton University, Princeton, 08544 New Jersey, USA

⁴Institute of Physics and Astronomy, University of Potsdam, 14476 Potsdam, Germany

⁵College of Engineering, Mathematics and Physical Sciences, University of Exeter,
Exeter, EX4 4QE, UK

⁶Georesilience Analytics, Leatherhead, UK

*Correspondences should be addressed to: nico.wunderling@pik-potsdam.de or jonathan.donges@pik-potsdam.de

4 **Current policies and actions make it very likely to, at least temporarily, over-**
5 **shoot the Paris climate targets of 1.5–<2.0°C above pre-industrial levels. If**
6 **this global warming range is exceeded, potential tipping elements such as the**
7 **Greenland Ice Sheet or Amazon rainforest may be at increasing risk of cross-**
8 **ing critical thresholds. This raises the question how much this risk is ampli-**
9 **fied by increasing overshoot magnitude and duration. Here, we investigate the**
10 **danger for tipping under a range of temperature overshoot scenarios using**
11 **a stylised network model of four interacting climate tipping elements. Our**
12 **model analysis reveals that temporary overshoots can increase tipping risks**
13 **by up to 72% compared to non-overshoot scenarios, even when the long-term**
14 **equilibrium temperature stabilises within the Paris range. Our results sug-**
15 **gest that avoiding high-end climate risks are only possible for low temperature**
16 **overshoots and if long-term temperatures stabilise at or below today’s levels of**
17 **global warming.**

18 It has long been proposed that important continental-scale subsystems of the Earth's climate
19 system possess nonlinear behaviour^{1,2}. The defining property of these tipping elements are their
20 self-perpetuating feedbacks once a critical threshold is transgressed³ such as the melt-elevation
21 feedback for the Greenland Ice Sheet⁴ or the moisture recycling feedback for the Amazon rain-
22 forest⁵. The global mean surface temperature has been identified as the driving parameter for
23 the state of the climate tipping elements^{6,7,1}, which include, among others, systems like the
24 large ice sheets on Greenland and Antarctica, the Atlantic Meridional Overturning Circulation
25 (AMOC), and the Amazon rainforest^{8,9,10,11}.

26 Besides further amplifying anthropogenic global warming³, the disintegration of such climate
27 tipping elements individually would have large consequences for the biosphere and human soci-
28 eties, including large-scale sea-level rise or biome collapses. Since the first mapping of climate
29 tipping elements in 2008¹ the scientific focus has increased, with a 2019 warning that nine of the
30 15 known climate tipping elements are showing signs of instability¹², followed by a listing of all
31 known climate tipping elements with expert judgements of tipping point confidence levels in the
32 IPCC AR6 WG1¹³. While the uncertainty for crossing tipping points is still stated as medium
33 to high, the IPCC concludes that crossing them triggering potentially abrupt changes cannot
34 be excluded from projected future global warming trajectories¹³. As this science has advanced
35 over the last two decades, potential temperature thresholds have been corrected downwards sev-
36 eral times¹². The most recent scientific assessment places the critical threshold temperatures of
37 triggering tipping points at 1–5°C, with moderate risks already at 1.5–2°C for several systems,
38 like the Greenland and West Antarctic Ice Sheets⁶. In this sense, tipping elements research pro-
39 vides even further scientific support to hold global mean surface temperatures within the Paris
40 range of well below 2°C, while at the same time emphasising that tipping point risks cannot be
41 ruled out even at this lower temperature range^{6,7}. There is thus a triple dilemma emerging here.
42 First, insufficient policies and actions mean that the world is following a trajectory well-beyond

43 2°C by the end of this century¹⁴. Second, essentially all IPCC scenarios that hold the 1.5°C line
44 include a period of several decades of temperature overshoot^{15,16,13}. And third, although given
45 the large uncertainties among the different assessments^{13,17}, research cannot exclude the cross-
46 ing of tipping point thresholds already at low temperature rise⁶. Therefore, more knowledge is
47 urgently needed on which overshoots still allow for low tipping risks^{18,19,20}.
48 Hence, it is essential to assess temperature overshoots and long-term temperature stabilisa-
49 tion levels that can lead to irreversible changes in the climate system. While the impacts of
50 overshoots have been investigated from a mathematical point of view and for individual cli-
51 mate tipping elements^{21,18,22}, they interact across scales in space and time, creating risks for
52 additional feedback dynamics^{12,23,24,25}. Interactions may increase tipping risks by triggering
53 cascades, when a transition of one element triggers transitions of connected tipping elements²⁶.
54 Therefore in this work, we combine interactions between climate tipping elements and temper-
55 ature overshoots in a stylised network model. We designed (stylised) our model to be able to
56 perform tipping risk assessments, but it should not be used to make predictions. We systemat-
57 ically assess the risk for tipping and identify a high climate risk zone, considering remaining
58 uncertainties in the properties of the tipping elements and different global warming overshoot
59 scenarios if Paris temperature targets are not met without overshoots.

60

61 **Modelling approach**

62 Following Wunderling et al. (2021)²⁶, we use a stylised network model of four coupled ordinary
63 differential equations designed for the analysis of risk assessments, which couples four climate
64 tipping elements (see Methods): the Greenland Ice Sheet, West Antarctic Ice Sheet, AMOC,
65 and Amazon rainforest (Fig. 1c). We assume that each of the four elements is a climate tip-
66 ping element, exhibiting a critical transition at its respective critical temperature threshold (see
67 Methods, Eq. 1)^{6,27}. Even though there is considerable uncertainty in complex climate mod-

68 els whether and at which global warming level the exact tipping point is located^{13,17}, evidence
69 from models of varying complexity, data based approaches and paleo-climate observations are
70 consistent with considerable risks for nonlinearities among them⁶ (SI chapter 1). On the other
71 hand, there are negative feedbacks, such as the Planck feedback, CO₂-fertilisation, ocean sol-
72 ubility of CO₂, and ocean heat uptake that stabilise the climate system^{13,28,29}. Those negative
73 feedbacks, generally well represented already in climate models (as compared to the tipping
74 elements explored in this paper), might modify the tipping properties of some tipping elements.
75 For example, the positive ice-albedo feedback despite competition with the negative Planck
76 feedback has been shown to induce two stable large-scale Earth system states, a snowball Earth
77 and a warm state^{30,31}. On the smaller scale of climate tipping elements, the Planck feedback
78 would be large if the global mean temperature increase from disintegrating climate tipping ele-
79 ments is large because the Planck feedback operates on the global mean temperature. At least
80 for the large ice sheets on Greenland and West Antarctica, however, this effect may be limited
81 since their complete disappearance would lead to a global warming of less than 0.2°C in total³².
82 On the other side, although the Amazon rainforest is stated to lose resilience³³, the formation
83 of spatial patterns^{34,35} and climate change may not affect all parts of the Amazon rainforest
84 equally³⁶ and could prevent a single system-wide tipping event.
85 Nevertheless, we argue that sufficient evidence exists for climate tipping points to justify a
86 risk analysis approach based on the precautionary principle. It is important to quantify tipping
87 risks because the likelihood of tipping points existing is nonzero, and if they exist, they present
88 high climate risks for the biosphere and human societies^{6,12}. This has been re-emphasised in
89 a recent study remarking that current risk assessments of high-end climate change scenarios
90 (including tipping elements) are dangerously underexplored^{37,38}. Simplified representations of
91 more complex phenomena is a useful modelling approach in this context for capturing broad-
92 scale patterns and risks.

93 Since the four tipping elements are not individual subsystems, we conceptualise the interac-
94 tions as linear couplings in our model (Eq. 1). Each of these interactions has a driving physical
95 mechanism behind it (Fig. 1c), which was coarsely quantified by a formalised expert elicita-
96 tion²⁵. While these interaction estimates were coarse, newer literature confirms and substan-
97 tiates them^{26,39,40,41}, enabling us to assess cascading tipping risks at a certain level of global
98 warming. For further details on the exact nature of the interactions see Fig. 1c and Wunderling
99 et al. (2021)²⁶.

100 Overall, our network model is able to capture the main dynamics of these four interacting tip-
101 ping elements, and is therefore able to propagate important uncertainties in the input param-
102 eters. It is designed to assess the risk for critical transitions, but can as such not be used for
103 predictions, nor to assess whether tipping points exist or not, but their existence is an a-priori
104 assumption in this work. Important model uncertainties include critical temperature thresholds,
105 interaction strengths and interaction network structures, as well as typical transition time scales
106 of individual tipping elements (see Methods and Tab. S1). Here, the transition time scale is the
107 time that is needed for a transition from the baseline to the transitioned regime for an individual
108 (non-interacting) climate tipping element as compiled in recent literature (cf. Fig. 1)⁶. The low
109 computational complexity of our approach allows to sample the parameter space by means of a
110 very large-scale Monte Carlo ensemble, including approximately 4.455 million individual en-
111 semble members in total. For the construction of the ensemble, but also for the boundary values
112 of the parameters uncertainties (based on the latest literature review⁶), see Methods. Lastly,
113 there is not only uncertainty in model parameters, but also in the assumed (fold-bifurcation)
114 structure of the tipping elements themselves due to negative feedbacks, at different strengths,
115 modifying the bifurcation structure. This uncertainty can be taken into account by altering the
116 prefactors of the cubic and linear terms of Eq. 1. Therefore, it would be possible to probe
117 scenarios where some of the tipping elements are weak (or not) nonlinear systems. However,

118 since exact values for these prefactors cannot be straightforwardly derived from existing data,
119 such a sensitivity assessment is beyond the scope of this work. More importantly, our present
120 study focuses on the high-end risk case where all considered climate subsystems possess tipping
121 points.

122 In our numerical experiments, the four tipping element network is exposed to different global
123 warming overshoot scenarios characterised by peak temperature, overshoot duration, and the
124 final convergence temperature reached in long-term equilibrium (Fig. 1a). All these important
125 properties of the overshoot trajectory determine the potential of a tipping event. The stylised
126 temperature overshoot trajectories applied to the four interacting climate tipping elements, were
127 primarily designed to capture typical temperature profiles generated by Earth System Model
128 simulations for low to medium emission scenarios⁴². Moreover, the formulation of the trajec-
129 tories allows for flexibility in how society manages the transition from current warming to the
130 convergence temperature, which can therefore lead to overshoot trajectories¹⁸. To this end, our
131 ensemble spans all combinations of (i) peak temperatures $T_{\text{Peak}} = 2.0, 2.5, \dots, 6.0^\circ\text{C}$ (maximally
132 reached temperature), (ii) convergence temperatures $T_{\text{Conv}} = 0.0, 0.5, \dots, 2.0^\circ\text{C}$ (final stabilisa-
133 tion temperature), and (iii) convergence times $t_{\text{Conv}} = 100, 200, \dots, 1000$ years (time to reach
134 T_{Conv}), allowing us to quantify the respective risk and time scale for tipping events. Note that
135 the limit case of $T_{\text{Peak}} = T_{\text{Conv}} = 2.0^\circ\text{C}$ is simulated as constant temperature. In this paper, we
136 will focus on peak temperatures up to 4.0°C , where 4.0°C represents an upper temperature limit
137 we investigate, based on *policies and targets* following COP26 and the climate-action-tracker¹⁴.
138 High-end warming scenarios with peak temperatures of $4.5\text{--}6.0^\circ\text{C}$ are added in the [Extended](#)
139 [Data figure material](#), which allow computing a comprehensive risk analysis. Fig. 1a presents
140 an exemplary timeline of an overshoot trajectory that peaks at 2.5°C warming and converges to
141 a 2.0°C convergence temperature after 400 years. The impact on the four studied interacting
142 tipping elements is shown in Fig. 1b (for further examples see Extended Data Fig. 1). In the

143 remainder of this work, the impact of a certain relevant parameter combination (T_{Peak} , T_{Conv} ,
144 t_{Conv}) on the risk of an element tipping is given by the fraction of all simulation runs that result
145 in the transitioned regime, averaged over all other parameters and uncertainties. We define the
146 tipping of an element as the tipping process being completed, i.e. when the tipping element
147 reaches the transitioned regime (cf. Fig. 1b). We first evaluate the tipping risk with respect to
148 the overshoot peak temperature, convergence temperature and convergence time, and identify
149 risk maps for a high climate risk zone. After that, we determine the mechanisms and reasons
150 for tipping events.

151

152 **The effects of overshoot peak temperature**

153 Focusing on the role of overshoot peak temperature, we find that the risk for the emergence of
154 at least one tipping event increases with rising peak temperature. Averaged over all ensemble
155 members, around one-third ($36.5 \pm 5.0\%$) of all simulations show a tipping event or cascade
156 at a peak temperature of 2.0°C , while it is close to three-quarters ($74.3 \pm 1.4\%$) of all simula-
157 tions at 4.0°C peak temperature (Fig. 2a). However, the dependence on the peak temperature
158 is unevenly distributed among the four different climate tipping elements (Fig. 2b). The tip-
159 ping risk for tipping elements with high inertia (slow tipping elements: Greenland and West
160 Antarctic Ice Sheets) remains relatively constant over an increasing peak temperature because
161 their reaction time (500–13,000 years) is slow against the duration of the overshoot trajectory
162 ($t_{\text{Conv}} = 100 - 1,000$ years). Therefore, the tipping risk for the Greenland Ice Sheet remains rel-
163 atively constant between $14.0 \pm 5.7\%$ ($T_{\text{Peak}} = 2.0^\circ\text{C}$) and $16.0 \pm 3.5\%$ ($T_{\text{Peak}} = 4.0^\circ\text{C}$, Fig. 2b).
164 In contrast, for tipping elements with low inertia (fast tipping elements: AMOC and Amazon
165 rainforest) there is a strong tipping risk increase, comparing $24.7 \pm 3.7\%$ ($T_{\text{Peak}} = 2.0^\circ\text{C}$) with
166 $50.8 \pm 4.4\%$ ($T_{\text{Peak}} = 4.0^\circ\text{C}$, Fig. 2b) for the AMOC. On the other hand, the tipping risk for
167 the slow tipping elements increases for increasing convergence times (Extended Data Fig. 3),

168 whereas the tipping risk for the fast tipping elements only increases slightly for increasing con-
169 vergence times above 200 years. This subsequent increase can largely be attributed to cascading
170 effects, where typically the Greenland Ice Sheet tipping has initiated tipping on the faster ele-
171 ments. Fig. 2 shows the equilibrium results after 50,000 simulation years, which demonstrate
172 the long-term commitment due to transgressed tipping thresholds. While this provides an im-
173 portant insight into potential locked-in change, some tipping risks are already realised after
174 100–1,000 years. On these shorter time scales, especially the AMOC and the Amazon rainfor-
175 est show a strong dependence on the peak temperature (Extended Data Fig. 2).

176

177 **Risk maps for identifying a high climate risk zone**

178 For final convergence temperatures comparable with today’s levels of warming (approx. $T_{\text{Conv}} =$
179 1.0°C), we find that the expected number of tipped elements is at least $\langle \# \rangle_{\text{tipped, min}} = 0.29$
180 (Fig. 3a). This minimal number of tipped elements is evaluated for the most optimistic case of
181 this study (lowest-left parameter combination in Fig. 3), where the peak temperature reaches
182 2.0°C above pre-industrial and the convergence time is 100 years. The tipping risk that at least
183 one tipping element transitions to its alternative state (related to $\langle \# \rangle_{\text{tipped, min}} = 0.29$) is 15%
184 (Fig. 3d). Stabilising global warming at the lower (upper) limit of the Paris range at 1.5°C
185 (2.0°C) above pre-industrial levels, increases the number of minimally tipped elements (to 1.19
186 and 1.89, Fig. 3b, c).

187 We define a *high climate risk zone* as the region, where the likelihood for no tipping event is
188 smaller than 66%, or the risk that one or more elements tip is higher than 33%. We compute this
189 risk and find a marked increase for increasing convergence temperatures (compare Fig. 3d, e, f).
190 For convergence temperatures of 1.5°C and above, our results indicate that the high climate
191 risk zone spans the entire state space for final convergence temperatures of $1.5\text{--}2.0^{\circ}\text{C}$. Only if
192 final convergence temperatures are limited to, or better below, today’s levels of global warming,

193 while peak temperatures are below 3.0°C, the tipping risks remain below 33% (Fig. 3d). In
194 parallel, the equipotential lines shift strongly from higher peak temperatures and convergence
195 times to lower ones with increasing convergence temperature. This leads to a lower likelihood of
196 low-risk scenarios without tipping elements transitioning to their alternative state. In the worst
197 case of a convergence temperature of 2.0°C (Fig. 3f), the tipping risk for at least one tipping
198 event to occur is on the order of above 90% if peak temperatures of 4.0°C are not prevented.
199 The devastating negative consequences of such a scenario with high likelihood of triggering
200 tipping events would entail significant sea level rise, biosphere degradation or considerable
201 North Atlantic temperature drops.

202 Therefore, this would entail an *unsafe overshoot* regime. On the other hand, strictly lowering
203 the final convergence temperature to or below today's levels of global warming while limiting
204 peak overshoot temperatures to 3.0°C and convergence times in parallel significantly reduces
205 the risk of tipping events (Extended Data Fig. 4 and Fig. 3d). In the most optimistic scenario,
206 tipping risks are kept below 5%.

207

208 **Tipping mechanisms under warming overshoots**

209 The risk for tipping events increases with higher peak temperatures, higher convergence tem-
210 peratures, and longer convergence times. However, the mechanism causing a tipping event in
211 our model is twofold: (i) The element tips due to the final temperature T_{Conv} being higher than
212 its critical temperature threshold. We call this *baseline tipping* because the final baseline (T_{Conv})
213 is already higher than the critical temperature (e.g. Fig. 1a,b for the Greenland Ice Sheet). (ii)
214 The element tips due to the temperature overshoot trajectory, which temporarily transgresses its
215 critical temperature threshold. We call this *overshoot tipping* (e.g. Extended Data Fig. 1c for
216 AMOC). In both cases, baseline or overshoot tipping, the first tipped element can draw along
217 other elements in a cascade such that the size of the cascade is not necessarily restricted to one.

218 Our results show that the risk for tipping events in scenarios converging within the limits of
219 the Paris climate target, ranges from 57.8% to 91.4% (Fig. 4). For small peak temperatures
220 ($T_{\text{Peak}} = 2.5^{\circ}\text{C}$), overshoot tipping only accounts for as little as 9% of all tipping events but
221 for higher peak temperature levels ($T_{\text{Peak}} = 4.0^{\circ}\text{C}$) this number can increase to as much as
222 42% (bar charts in Fig. 3). Specifically, the risk of tipping increases between 10–72% in these
223 scenarios for overshooting before stabilising at the convergence temperature as compared to
224 non-overshoot scenarios. Note that in the special case, where the peak temperature equals the
225 convergence temperature ($T_{\text{Peak}} = T_{\text{Conv}} = 2.0^{\circ}\text{C}$), overshoot tipping events do not occur.

226 The number of expected tipping events increases from short to long time scales as tested in our
227 experiments, where we separated tipping events realised after 100 (short-term tipping), 1,000
228 (mid-term tipping) and 50,000 simulation years (equilibrium tipping, pie charts in Fig. 4). For
229 higher peak temperatures, we additionally observe a larger portion of tipping events realised
230 within 100 and 1,000 years. These short-term events are dominantly caused by the fast tipping
231 elements (AMOC and Amazon rainforest), but mid-term events are additionally also partially
232 caused by a tipping West Antarctic Ice Sheet (Extended Data Fig. 2). Together our results
233 indicate that, in order to avoid tipping events within the Paris range, not only the peak temper-
234 ature must be limited but also the final convergence temperature has to fall significantly below
235 1.5°C in the long run (Figs. 3 and Extended Data Fig. 7). To further hedge tipping risks, the
236 time to reach the convergence temperature must also be small (i.e. $t_{\text{Conv}} \lesssim 200$ yrs, cf. Ex-
237 tended Data Fig. 4c,d). However, current *policies and action* would lead to 2.0 – 3.6°C (mean:
238 2.7°C), and present *pledges and targets* to 1.7 – 2.6°C (mean: 2.1°C) above pre-industrial, based
239 on the COP26-update published in November 2021 as expected temperatures in 2100 (see cli-
240 mateactiontracker and vertical axis in Fig. 4c)¹⁴. As noted above, these temperatures would
241 lead to significant tipping risks if they were interpreted as peak temperatures. If they would
242 be convergence temperatures, tipping very likely is unavoidable. Additionally, high-end sce-

243 nario simulations with very high peak temperatures between 4.5–6.0°C reveal that the risk to
244 observe tipping becomes virtually certain ($>95\%$ for $T_{\text{Peak}} \gtrsim 5.5^\circ\text{C}$). At these scenarios, it is
245 likely ($>40\%$) that the first tipping event would occur within 100 years, typically the Amazon
246 rainforest or AMOC (Extended Data Fig. 8).

247

248 Furthermore, we investigate the effects of interactions between the tipping elements on the risk
249 of (cascading) transitions in overshoot scenarios (SI chapter 2 and Fig. S1). Our results show
250 that increasing the interaction strength from 0.0 (no interaction) to 0.3 increases the average
251 number of tipped elements strongly (by $49.3 \pm 2.1\%$) at a convergence temperature of 2.0°C . A
252 further increase of the interaction strength from 0.3, only leads to a marginal additional tipping
253 risk (of $12.1 \pm 0.5\%$, Fig. S1e).

254

255 **Discussion**

256 In summary, we find that in our stylised network model the high climate risk zone characterised
257 by large tipping risks ($>33\%$) can only be avoided if several aspects are met in parallel due to
258 the different time scales involved. These aspects are limited overshoot peak temperatures, lim-
259 ited convergence times, and most importantly limited convergence temperatures (due to baseline
260 tipping) to a level of, or better, below the current level of global warming (1.2°C)¹⁴. Our model
261 analysis shows that the overshoot peak temperature should be constrained based on fast tipping
262 elements (Fig. 2b), whereas slow tipping elements largely determine the upper limit for conver-
263 gence times (Extended Data Fig. 3). The convergence temperature needs to be limited to avoid
264 baseline tipping, and lower levels of it will also assist in avoiding overshoot tipping (Fig. 4).
265 Therefore, the combination of the slow Greenland Ice Sheet having a low temperature threshold
266 and the faster elements (AMOC, Amazon rainforest) having at least partially higher thresholds
267 (Tab. S1), facilitates the possibility of a small overshoot without causing tipping events and

268 thus further cascades. Ritchie et al. (2021)¹⁸ came to similar conclusions for individual tip-
269 ping elements but we find, for a sufficient interaction strength (≥ 0.2), a marked increase in the
270 expected number of tipped elements in equilibrium due to the possibility of emerging tipping
271 cascades (Fig. S1). Taken together, safe and unsafe temporary overshoot trajectories can clearly
272 be separated.

273 The choices of our stylised global warming overshoot scenarios are motivated by current knowl-
274 edge, summarising short and long-term effects. The shape of the short-term overshoot trajec-
275 tories captures the temperature profiles from different Earth system model simulations⁴², but is
276 still of conceptualised nature (Eq. 2). To allow for a direct comparison to the baseline critical
277 temperatures, we keep the temperature trajectories at constant levels in the long run. While
278 this is supported by ZECMIP (Zero Emissions Commitment Model Intercomparison Project)
279 for the near- to intermediate future for decades to centuries^{43,44}, it is unclear how carbon sinks
280 and sources behave for the more distant future. On time scales of centuries to millennia, it
281 seems more likely than not that a slight downward trend of global mean temperatures will be
282 entered^{44,45,46}. Still, large uncertainties remain and make future research necessary as has for
283 instance been proposed by using a novel framework of model experiments for zero emission
284 simulations⁴⁷. Overall, it is questionable whether naturally decreasing temperatures would be
285 sufficient to bring global mean temperatures after an overshoot back down to safe levels without
286 additional artificial carbon removal from the atmosphere⁴⁶.

287 Our employed stylised network model does not directly capture physical processes or the spa-
288 tial extent of tipping elements (e.g. important for spatial heterogeneity), and can as such not
289 be used as a model for predictions, but has been designed as a risk assessment tool for some
290 of the potentially most nonlinear and societally harmful elements in the Earth system. Thus,
291 a benefit of low complexity models such as ours is that they allow for very large-scale Monte
292 Carlo ensemble simulations, which can take into account relevant uncertainties, e.g., in interac-

293 tion structure, strength and critical temperature thresholds. Still, future research should also be
294 targeted at building more complex models around coupled nonlinear phenomena and climate
295 tipping elements, either by combining simple physics-based models and combining those mod-
296 els with observational data^{48,49,50,51}, or by employing Earth System Models of either intermedi-
297 ate or high complexity. In the latter case, tipping elements could be spatially resolved, which
298 might refine or modify some of the results gained here³⁵. Moreover, data-based approaches
299 or machine learning should be considered, with which it might be possible to reconstruct ac-
300 tual interaction strength values^{17,52}. Recently, it has also been proposed to combine these two
301 research strands to what has been framed “neural” Earth system models⁵³. Also, uncertainty
302 in the assumed fold-bifurcation structure should be taken into account in future work to probe
303 how results are affected if some of the tipping elements were less nonlinear, e.g. due to spa-
304 tial pattern formation or negative feedbacks^{28,34,35}. Most importantly, this would decrease the
305 abruptness of change expected in the model, or may increase the time for complete disintegra-
306 tion of the respective (tipping) element. Thus, the convergence time for safe overshoots would
307 likely be larger.

308 Even in the absence of climate tipping points, future climate change will cause significant eco-
309 nomic, ecological and societal damage, however, the need for climate action becomes even
310 more urgent if (interacting) climate tipping elements would undergo a critical transition during
311 an overshoot^{54,55,56}. Critically, to reduce the risk and prevent the negative impacts of interacting
312 climate tipping elements on human societies and biosphere integrity, it is of utmost importance
313 to ensure that temperature overshoot trajectories are limited in both magnitude and duration,
314 while stabilising global warming at, or better, below the Paris agreement’s targets. Further-
315 more, also many of the low global mean temperature scenarios, limiting warming to well-below
316 2°C above pre-industrial levels, are forced to include an overshoot period over 1.5°C^{57,58}. Our
317 paper highlights the importance to investigate further the risks of triggering non-linear changes

318 also during these lower and shorter overshoots in future work. Although our results motivate
319 that a future climate trajectory without or with limited temperature overshoots would be prefer-
320 able, current results from the COP conferences and their pledges and targets indicate that at least
321 temporary overshoots over the Paris range seem likely^{14,59}. This would not only be problematic
322 because of natural risks exerted by the potential of disintegrating climate tipping elements, but
323 also economic damages would be smaller in case of a non-overshoot scenario^{59,60}.

324

325 **Data availability.** The data on overshoot trajectories and time series of the 4.455 million indi-
326 vidual ensemble members are, due to the very high storage requirements, available from N.W.
327 upon reasonable request. The code that led to these results is freely available (see code avail-
328 ability statement).

329

330 **Code availability.** The code leading to the overshoot trajectories and tipping risk assess-
331 ments is available within the python modelling package *pycascades* at [https://pypi.org/
332 project/pycascades/](https://pypi.org/project/pycascades/), together with a model description paper⁶¹. The version of *pycas-*
333 *cad*es of the results of this manuscript is stored together with a readme, code of the figure files
334 and intermediate evaluation scripts under the doi: . In case of questions, requests or required
335 assistance, please contact N.W..

336

337 **Acknowledgements**

338 This work has been carried out within the framework of PIK's FutureLab on Earth Resilience
339 in the Anthropocene. N.W., J.R., and J.F.D. acknowledge support from the European Research
340 Council Advanced Grant project ERA (Earth Resilience in the Anthropocene, ERC-2016-ADG-
341 743080). J.F.D. is grateful for financial support by the project CHANGES funded by the Fed-
342 eral Ministry for Education and Research (BMBF) within the framework "PIK_Change" under

343 grant 01LS2001A. R.W., J.R., D.I.A.M., S.L. and B.S. acknowledge financial support via the
344 Earth Commission, hosted by FutureEarth. The Earth Commission is the science component
345 of the Global Commons Alliance, a sponsored project of Rockefeller Philanthropy Advisors,
346 with support from Oak Foundation, MAVA, Porticus, Gordon and Betty Moore Foundation,
347 Herlin Foundation and the Global Environment Facility. The Earth Commission is also sup-
348 ported by the Global Challenges Foundation. P.D.L.R. acknowledges support from the Euro-
349 pean Research Council ‘Emergent Constraints on Climate-Land feedbacks in the Earth System
350 (ECCLES)’ project, grant agreement number 742472. The authors gratefully acknowledge the
351 European Regional Development Fund (ERDF), the BMBF and the Land Brandenburg for sup-
352 porting this project by providing resources on the high performance computer system at the
353 Potsdam Institute for Climate Impact Research.

354

355 **Author contributions**

356 R.W., J.R. and J.F.D. conceived the study. N.W. designed the study, performed the simulations
357 and led the writing of the manuscript with input from all authors. N.W., S.L. and B.S. prepared
358 the figures with input from R.W., J.R. and J.F.D.. J.F.D. led the supervision of this study.

359

360 **Competing interests**

361 The authors declare no competing interests.

References

1. Lenton, T. M. *et al.* Tipping elements in the Earth's climate system. *Proceedings of the National Academy of Sciences* **105**, 1786–1793 (2008).
2. Schellnhuber, H. J. Tipping elements in the Earth System. *Proceedings of the National Academy of Sciences* **106**, 20561–20563 (2009).
3. Steffen, W. *et al.* Trajectories of the Earth System in the Anthropocene. *Proceedings of the National Academy of Sciences* **115**, 8252–8259 (2018).
4. Levermann, A. & Winkelmann, R. A simple equation for the melt elevation feedback of ice sheets. *The Cryosphere* **10**, 1799–1807 (2016).
5. Aragão, L. E. The rainforest's water pump. *Nature* **489**, 217–218 (2012).
6. Armstrong McKay, D. I. *et al.* Exceeding 1.5°C global warming could trigger multiple climate tipping points. *Science* **377**, eabn7950 (2022).
7. Schellnhuber, H. J., Rahmstorf, S. & Winkelmann, R. Why the right climate target was agreed in Paris. *Nature Climate Change* **6**, 649–653 (2016).
8. Garbe, J., Albrecht, T., Levermann, A., Donges, J. F. & Winkelmann, R. The hysteresis of the Antarctic ice sheet. *Nature* **585**, 538–544 (2020).
9. Robinson, A., Calov, R. & Ganopolski, A. Multistability and critical thresholds of the Greenland ice sheet. *Nature Climate Change* **2**, 429–432 (2012).
10. Hawkins, E. *et al.* Bistability of the Atlantic overturning circulation in a global climate model and links to ocean freshwater transport. *Geophysical Research Letters* **38** (2011).

- 382 11. Nobre, C. A. & Borma, L. D. S. ‘Tipping points’ for the Amazon forest. *Current Opinion*
383 *in Environmental Sustainability* **1**, 28–36 (2009).
- 384 12. Lenton, T. M. *et al.* Climate tipping points—too risky to bet against. *Nature* **575**, 592–595
385 (2019).
- 386 13. Masson-Delmotte, V. P. *et al.* *IPCC, 2021: Climate Change 2021: The Physical Science*
387 *Basis. Contribution of Working Group I to the Sixth Assessment Report of the Intergovern-*
388 *mental Panel on Climate Change* (Cambridge University Press, 2021).
- 389 14. Climate Analytics, New Climate Institute, The Climate Action Tracker Ther-
390 mometer (2021). URL [https://climateactiontracker.org/global/](https://climateactiontracker.org/global/cat-thermometer/)
391 [cat-thermometer/](https://climateactiontracker.org/global/cat-thermometer/).
- 392 15. Meinshausen, M. *et al.* Realization of Paris Agreement pledges may limit warming just
393 below 2°C. *Nature* **604**, 304–309 (2022).
- 394 16. Schleussner, C.-F., Ganti, G., Rogelj, J. & Gidden, M. J. An emission pathway classification
395 reflecting the Paris Agreement climate objectives. *Communications Earth & Environment* **3**,
396 1–11 (2022).
- 397 17. Drijfhout, S. *et al.* Catalogue of abrupt shifts in intergovernmental panel on climate change
398 climate models. *Proceedings of the National Academy of Sciences* **112**, E5777–E5786
399 (2015).
- 400 18. Ritchie, P. D., Clarke, J. J., Cox, P. M. & Huntingford, C. Overshooting tipping point
401 thresholds in a changing climate. *Nature* **592**, 517–523 (2021).
- 402 19. Tong, D. *et al.* Committed emissions from existing energy infrastructure jeopardize 1.5°C
403 climate target. *Nature* **572**, 373–377 (2019).

- 404 20. Raftery, A. E., Zimmer, A., Frierson, D. M., Startz, R. & Liu, P. Less than 2°C warming by
405 2100 unlikely. *Nature Climate Change* **7**, 637–641 (2017).
- 406 21. Ritchie, P., Karabacak, Ö. & Sieber, J. Inverse-square law between time and amplitude for
407 crossing tipping thresholds. *Proceedings of the Royal Society A* **475**, 20180504 (2019).
- 408 22. Alkhayuon, H., Ashwin, P., Jackson, L. C., Quinn, C. & Wood, R. A. Basin bifurcations,
409 oscillatory instability and rate-induced thresholds for Atlantic Meridional Overturning Cir-
410 culation in a global oceanic box model. *Proceedings of the Royal Society A* **475**, 20190051
411 (2019).
- 412 23. Rocha, J. C., Peterson, G., Bodin, Ö. & Levin, S. Cascading regime shifts within and across
413 scales. *Science* **362**, 1379–1383 (2018).
- 414 24. Lenton, T. M. & Williams, H. T. On the origin of planetary-scale tipping points. *Trends in*
415 *Ecology & Evolution* **28**, 380–382 (2013).
- 416 25. Kriegler, E., Hall, J. W., Held, H., Dawson, R. & Schellnhuber, H. J. Imprecise probability
417 assessment of tipping points in the climate system. *Proceedings of the National Academy of*
418 *Sciences* **106**, 5041–5046 (2009).
- 419 26. Wunderling, N., Donges, J. F., Kurths, J. & Winkelmann, R. Interacting tipping elements
420 increase risk of climate domino effects under global warming. *Earth System Dynamics* **12**,
421 601–619 (2021).
- 422 27. Bathiany, S. *et al.* Beyond bifurcation: using complex models to understand and predict
423 abrupt climate change. *Dynamics and Statistics of the Climate System* **1** (2016).
- 424 28. Goosse, H. *et al.* Quantifying climate feedbacks in polar regions. *Nature Communications*
425 **9**, 1–13 (2018).

- 426 29. Soden, B. J. & Held, I. M. An assessment of climate feedbacks in coupled ocean-
427 atmosphere models. *Journal of Climate* **19**, 3354–3360 (2006).
- 428 30. Lucarini, V. & Bódai, T. Transitions across melancholia states in a climate model: Recon-
429 ciling the deterministic and stochastic points of view. *Physical Review Letters* **122**, 158701
430 (2019).
- 431 31. Margazoglou, G., Grafke, T., Laio, A. & Lucarini, V. Dynamical landscape and multista-
432 bility of a climate model. *Proceedings of the Royal Society A* **477**, 20210019 (2021).
- 433 32. Wunderling, N., Willeit, M., Donges, J. F. & Winkelmann, R. Global warming due to loss
434 of large ice masses and Arctic summer sea ice. *Nature Communications* **11**, 1–8 (2020).
- 435 33. Boulton, C. A., Lenton, T. M. & Boers, N. Pronounced loss of Amazon rainforest resilience
436 since the early 2000s. *Nature Climate Change* **12**, 271–278 (2022).
- 437 34. Bastiaansen, R., Dijkstra, H. A. & von der Heydt, A. S. Fragmented tipping in a spatially
438 heterogeneous world. *Environmental Research Letters* **17**, 045006 (2022).
- 439 35. Rietkerk, M. *et al.* Evasion of tipping in complex systems through spatial pattern formation.
440 *Science* **374**, eabj0359 (2021).
- 441 36. Wunderling, N. *et al.* Recurrent droughts increase risk of cascading tipping events by out-
442 pacing adaptive capacities in the Amazon rainforest. *Proceedings of the National Academy*
443 *of Sciences* **119**, e2120777119 (2022).
- 444 37. Kemp, L. *et al.* Climate Endgame: Exploring catastrophic climate change scenarios. *Pro-*
445 *ceedings of the National Academy of Sciences* **119**, e2108146119 (2022).
- 446 38. Jehn, F. U. *et al.* Focus of the IPCC assessment reports has shifted to lower temperatures.
447 *Earth's Future* **10**, e2022EF002876 (2022).

- 448 39. Weijer, W. *et al.* Stability of the atlantic meridional overturning circulation: A review and
449 synthesis. *Journal of Geophysical Research: Oceans* **124**, 5336–5375 (2019).
- 450 40. Jackson, L. *et al.* Global and European climate impacts of a slowdown of the AMOC in a
451 high resolution GCM. *Climate Dynamics* **45**, 3299–3316 (2015).
- 452 41. Mitrovica, J. X., Gomez, N. & Clark, P. U. The sea-level fingerprint of West Antarctic
453 collapse. *Science* **323**, 753–753 (2009).
- 454 42. Huntingford, C. *et al.* Flexible parameter-sparse global temperature time profiles that sta-
455 bilise at 1.5 and 2.0°C. *Earth System Dynamics* **8**, 617–626 (2017).
- 456 43. Jones, C. D. *et al.* The Zero Emissions Commitment Model Intercomparison Project
457 (ZECMIP) contribution to C4MIP: quantifying committed climate changes following zero
458 carbon emissions. *Geoscientific Model Development* **12**, 4375–4385 (2019).
- 459 44. MacDougall, A. H. *et al.* Is there warming in the pipeline? A multi-model analysis of the
460 Zero Emissions Commitment from CO₂. *Biogeosciences* **17**, 2987–3016 (2020).
- 461 45. Williams, R. G., Roussenov, V., Frölicher, T. L. & Goodwin, P. Drivers of continued
462 surface warming after cessation of carbon emissions. *Geophysical Research Letters* **44**, 10–
463 633 (2017).
- 464 46. Zickfeld, K. *et al.* Long-term climate change commitment and reversibility: An EMIC
465 intercomparison. *Journal of Climate* **26**, 5782–5809 (2013).
- 466 47. King, A. D. *et al.* Studying climate stabilization at Paris Agreement levels. *Nature Climate*
467 *Change* **11**, 1010–1013 (2021).
- 468 48. Dekker, M. M., Von Der Heydt, A. S. & Dijkstra, H. A. Cascading transitions in the climate
469 system. *Earth System Dynamics* **9**, 1243–1260 (2018).

- 470 49. Ciemer, C., Winkelmann, R., Kurths, J. & Boers, N. Impact of an AMOC weakening on the
471 stability of the southern Amazon rainforest. *The European Physical Journal Special Topics*
472 1–9 (2021).
- 473 50. Lohmann, J. & Ditlevsen, P. D. Risk of tipping the overturning circulation due to increasing
474 rates of ice melt. *Proceedings of the National Academy of Sciences* **118** (2021).
- 475 51. Sinet, S., Dijkstra, H. A. & Heydt, A. S. v. d. AMOC stabilization under the interaction
476 with tipping polar ice sheets (in review) (2022). URL [https://www.essoar.org/
477 doi/abs/10.1002/essoar.10511833.1](https://www.essoar.org/doi/abs/10.1002/essoar.10511833.1).
- 478 52. Runge, J. *et al.* Identifying causal gateways and mediators in complex spatio-temporal
479 systems. *Nature Communications* **6**, 1–10 (2015).
- 480 53. Irrgang, C. *et al.* Towards neural Earth system modelling by integrating artificial intelli-
481 gence in Earth system science. *Nature Machine Intelligence* **3**, 667–674 (2021).
- 482 54. Cai, Y., Lenton, T. M. & Lontzek, T. S. Risk of multiple interacting tipping points should
483 encourage rapid CO₂ emission reduction. *Nature Climate Change* **6**, 520–525 (2016).
- 484 55. Cai, Y., Judd, K. L., Lenton, T. M., Lontzek, T. S. & Narita, D. Environmental tipping
485 points significantly affect the cost- benefit assessment of climate policies. *Proceedings of
486 the National Academy of Sciences* **112**, 4606–4611 (2015).
- 487 56. Lemoine, D. & Traeger, C. P. Economics of tipping the climate dominoes. *Nature Climate
488 Change* **6**, 514–519 (2016).
- 489 57. Masson-Delmotte, V. *et al.* *An IPCC Special Report on the impacts of global warming of
490 1.5°C* (Cambridge University Press, 2018).

- 491 58. Schleussner, C.-F. *et al.* Science and policy characteristics of the Paris Agreement temper-
492 ature goal. *Nature Climate Change* **6**, 827–835 (2016).
- 493 59. Drouet, L. *et al.* Net zero-emission pathways reduce the physical and economic risks of
494 climate change. *Nature Climate Change* **11**, 1070–1076 (2021).
- 495 60. Riahi, K. *et al.* Cost and attainability of meeting stringent climate targets without overshoot.
496 *Nature Climate Change* **11**, 1063–1069 (2021).

497 **Methods**

498 **Interacting climate tipping elements model.** We use the stylised network model designed for
 499 risk analysis of four interacting tipping elements detailed in Wunderling et al. (2021)²⁶. Each
 500 tipping element is described by the following differential equation

$$\frac{dx_i}{dt} = \left[-x_i^3 + x_i + \sqrt{\frac{4}{27}} \cdot \frac{\Delta\text{GMT}(t)}{T_{\text{crit},i}} + d \cdot \sum_{\substack{j \\ j \neq i}} \frac{s_{ij}}{10} (x_j + 1) \right] \frac{1}{\tau_i}. \quad (1)$$

501 Here, x_i describes the state of the respective tipping element $i = \text{GIS}, \text{AMOC}, \text{WAIS}, \text{AMAZ}$
 502 (GIS: Greenland Ice Sheet, AMOC: Atlantic Meridional Overturning Circulation, WAIS: West
 503 Antarctic Ice Sheet, AMAZ: Amazon rainforest). This differential equation possesses two dif-
 504 ferent stable states: a baseline regime around $x_i \approx -1.0$ and a transitioned regime around
 505 $x_i \approx +1.0$. $\Delta\text{GMT}(t)$ denotes the global mean surface temperature increase above pre-
 506 industrial levels (as compared to the 1850–1900 level). This term is time dependent because
 507 of the time dependence of the overshoot trajectory, which serves as our input: $\Delta\text{GMT}(t) =$
 508 overshoot trajectory(t). The mathematical form of the overshoot trajectory is given below in
 509 the methods section: *temperature overshoot trajectories*. $T_{\text{crit},i}$ denotes the critical temperatures
 510 for the four tipping elements. The link strength values s_{ij} are taken from an expert elicita-
 511 tion²⁵, and each represent a physical mechanism (see Fig. 1c and Tab. S1). While these link
 512 strength values are quantified, the absolute importance of the interaction is not known for many
 513 of the interactions. Therefore, we introduce the interaction strength parameter d , which is var-
 514 ied between 0.0 and 1.0, where $d = 0.0$ means no interaction between the tipping elements
 515 and $d = 1.0$ means that interactions are approximately as important as the individual dynam-
 516 ics. With that we can probe a large range of possible interactions strengths among the tipping
 517 elements.

518 Lastly, the time scale-parameter τ_i denotes the transition time of a particular tipping element.
 519 Of course, the four stylised differential equations above (Eq. 1) are a strong simplification of

520 the more complex tipping elements. However, they represent a summary of the main stability
521 patterns, as has been argued in literature before^{26,27}. For more details on the mathematics in
522 this model, please be referred to Wunderling et al. (2021)²⁶. As initial conditions at $t = 0$,
523 the states of the four climate tipping elements are set to $x_i = -1.0$ (the completely untipped,
524 baseline regime), and the parameters for T_{crit} , s_{ij} , τ_i are chosen from their respective limits (see
525 Methods: *parameter uncertainties* and Tab. S1).

526

527 **Parameter uncertainties.** There are uncertainties in several parameters of the model (Eq. 1
528 and Tab. S1): (i) In the critical temperature regimes $T_{\text{crit}, i}$, which are taken from the recently re-
529 fined literature values⁶. (ii) The interactions between the climate tipping elements all represent
530 physical mechanisms behind each pair of tipping elements. For instance a melting Greenland
531 Ice Sheet induces a freshwater input into the North Atlantic and, by that, weakens the AMOC,
532 while a weakening AMOC would reduce the warming over Greenland (Fig. 1). There is a con-
533 siderable uncertainty of the link strength parameters s_{ij} , which are included in our uncertainty
534 analysis, and their values are taken from an expert elicitation on interacting climate tipping ele-
535 ments²⁵. The same values for interaction strengths have been used in earlier research on tipping
536 cascades²⁶. (iii) The upper and lower bounds for transition times for the four tipping elements
537 are again taken from recent literature⁶. It is important to note that the timescales for tipping
538 vary from decades, over centuries up to millennia depending on the respective tipping element.
539 While the Amazon rainforest and the AMOC tip on shorter timescales (decades to centuries),
540 the Greenland and West Antarctic Ice Sheets take longer to disintegrate (multiple centuries to
541 millennia). These, on at least two orders of magnitude, different transition times have important
542 effects on the dynamics of tipping, and as to whether a specific tipping event occurs or not.
543 These effects are discussed in the main text.

544

545 **Propagation of uncertainties via a Monte Carlo ensemble.** Since there are considerable un-
546 certainties in the critical temperature regimes, interaction strengths and structure, as well as in
547 the transition time scales, we set up a large-scale Monte Carlo ensemble to adequately propagate
548 the uncertainties in these parameters. The uncertainty range of the parameter uncertainties are
549 given in Tab. S1. For each combination of peak temperature ($T_{\text{Peak}} = 2.0, 2.5, \dots, 6.0^\circ\text{C}$), con-
550 vergence temperature ($T_{\text{Conv}} = 0.0, 0.5, \dots, 2.0^\circ\text{C}$), convergence time ($t_{\text{Conv}} = 100, 200, \dots, 1000$
551 years) and interaction strength ($d = 0.0, 0.1, \dots, 1.0$), we draw 100 realisations from a contin-
552 uous uniform distribution using a latin hypercube algorithm⁶² over the uncertainties in critical
553 temperatures, link strengths and transition times. This leads to $9 \cdot 5 \cdot 10 \cdot 11 \cdot 100 = 495,000$
554 ensemble members, which are looped over the 9 possible different network structures ([i] a
555 positive link between WAIS→AMOC and a positive link between AMOC→AMAZ, [ii] a zero
556 link between WAIS→AMOC and a positive link between AMOC→AMAZ, ..., [ix] a negative
557 link between WAIS→AMOC and a negative link between AMOC→AMAZ). With this proce-
558 dure, we obtain approximately 4.455 million ensemble members in total. By drawing from a
559 continuous uniform distribution for all tipping elements, we slightly overestimate the overall
560 uncertainties and perform a maximum uncertainty assessment. Therefore, our errors are con-
561 servative. After 100 years, 1,000 years and in equilibrium (here: 50,000 years), we branch off
562 the results for each of our 4.455 million ensemble members such that we can assess our results
563 at these three different timings.

564

565 **Temperature overshoot trajectories.** In this study, we have used stylised temperature over-
566 shoot trajectories based on overshoot trajectories that capture temperature profiles generated by
567 Earth System Model simulations for a low to medium emissions scenario⁴²:

$$\Delta\text{GMT}(t) = T_0 + \gamma t - [1 - e^{-(\mu_0 + \mu_1 t)t}] [\gamma t - (T_{\text{Conv}} - T_0)]. \quad (2)$$

568 In this equation, the temperature overshoot trajectory $\Delta\text{GMT}(t)$ is determined via five param-
569 eters: (i) T_0 is the approximate current level of global warming, i.e. the point at which the
570 trajectories start at $t = 0$. We have chosen $T_0 = 1.0^\circ\text{C}$ above pre-industrial levels. (ii) T_{Conv} is
571 the final convergence temperature, for which we have chosen an ensemble approach compris-
572 ing $T_{\text{Conv}} = 0.0, 0.5, 1.0, 1.5, 2.0^\circ\text{C}$ above pre-industrial. (iii) The parameter γ is chosen such
573 that the global warming rate matches the recent past. The exponential decay term describes the
574 development away from the linearly increasing trend (set by γ) bent towards the stabilisation
575 level (set by T_{Conv}), specified by the parameters (iv) μ_0 and (v) μ_1 . In our ensemble, we con-
576 struct a temperature overshoot trajectory with a specific peak temperature T_{Peak} and convergence
577 time t_{Conv} by iteratively altering the parameters γ , μ_0 and μ_1 until it matches the desired peak
578 temperature and convergence time. Exemplary overshoot trajectories can be found in Extended
579 Data Fig. 1, where the chosen parameters correspond to Fig. 1a. The chosen parameter values
580 to get $T_{\text{Peak}} = 2.5^\circ\text{C}$ and $t_{\text{Conv}} = 400$ years are: $\gamma = 0.0963^\circ\text{C yr}^{-1}$, $\mu_0 = 1.5 \cdot 10^{-3} \text{ yr}^{-1}$, and
581 $\mu_1 = 1.83 \cdot 10^{-4} \text{ yr}^{-2}$. The convergence temperature is set to $T_{\text{Conv}} = 2.0^\circ\text{C}$. The accuracy we
582 require for our scenarios is $\Delta T_{\text{Peak}} < 0.025^\circ\text{C}$ and $\Delta t_{\text{Conv}} < 0.5$ years, where the convergence
583 time is determined as the time when the temperature overshoot curve has reached the conver-
584 gence temperature to an accuracy of 0.01°C .

585

586 **Notes on maps.** This paper makes use of perceptually uniform colour maps developed by
587 F. Crameri⁶³. The underlying world map of Fig. 1 has been created by cartopy⁶⁴.

588

589 References

590 61. Wunderling, N. *et al.* Modelling nonlinear dynamics of interacting tipping elements on
591 complex networks: the PyCascades package. *The European Physical Journal Special Top-*

592 *ics* 1–14 (2021).

593 62. Baudin, M. pyDOE: The experimental design package for python. URL [https:](https://pythonhosted.org/pyDOE/index.html)
594 [//pythonhosted.org/pyDOE/index.html](https://pythonhosted.org/pyDOE/index.html).

595 63. Cramer, F. Geodynamic diagnostics, scientific visualisation and staglab 3.0. *Geoscientific*
596 *Model Development* **11**, 2541–2562 (2018).

597 64. Elson, P. *et al.* Cartopy: a cartographic python library with a matplotlib interface. zenodo
598 doi.org/10.5281/zenodo.7065949 (2022).

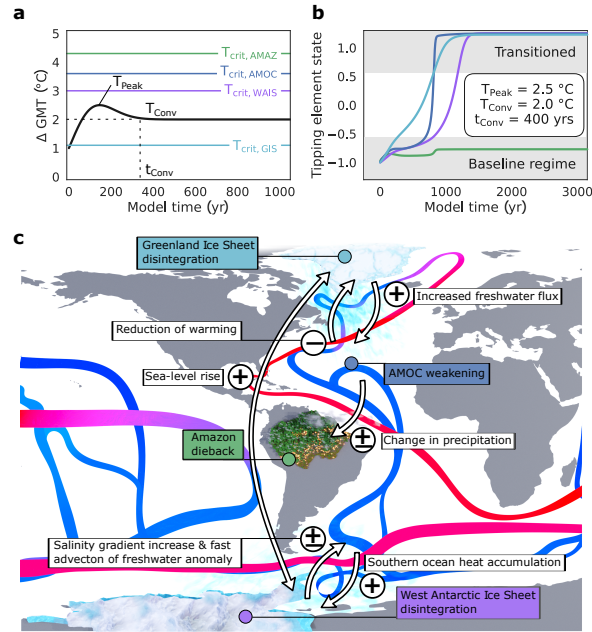


Fig. 1 | Interacting climate tipping elements. **a**, Exemplary global warming overshoot scenario with a peak temperature of $T_{\text{Peak}} = 2.5^{\circ}\text{C}$, a convergence temperature of $T_{\text{Conv}} = 2.0^{\circ}\text{C}$ above pre-industrial, and a time to convergence to 2.0°C of $t_{\text{Conv}} = 400$ years. This scenario is applied to a set of four interacting climate tipping elements with an exemplary draw of critical thresholds from their full uncertainty ranges (Tab. S1). **b**, The effect of the overshoot trajectory shown in panel a: the Greenland Ice Sheet, the West Antarctic Ice Sheet and the AMOC tip. The grey shaded areas depict the two possible states, either not tipped (baseline regime) or tipped state (transitioned). **c**, Map of the four interacting climate tipping elements. Each arrow represents a physical interaction mechanism between a pair of tipping elements, which can either be destabilising (denoted as +), stabilising (denoted as -), or unclear (denoted as +/-).

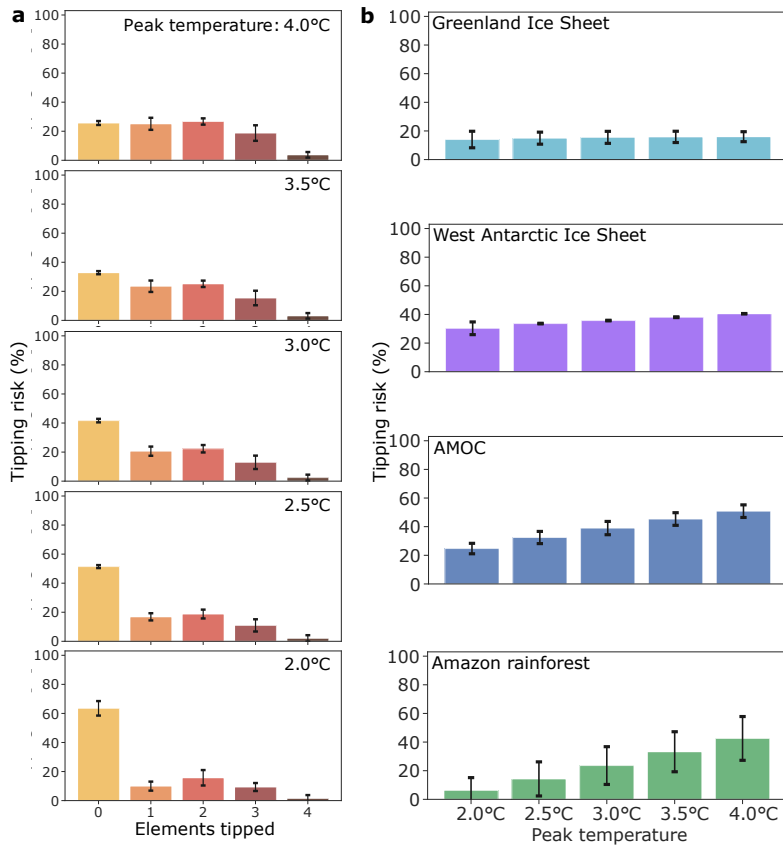


Fig. 2 | Effect of overshoot peak temperature. **a**, Number of tipped elements crossing tipping points due to additional forcing at overshoot peak temperatures of 2.0–4.0°C above pre-industrial levels. **b**, Risk for the individual climate tipping elements of transitioning into the undesired state crossing tipping points at overshoot peak temperatures of 2.0–4.0°C. We depict the average of the equilibrium run (long-term tipping after 50,000 simulation years) over the entire ensemble as the bar height and the error bars show the standard deviation. High-end overshoot peak temperatures up to 6.0°C above pre-industrial levels and transition times (after 100 yrs, 1,000 yrs, and in equilibrium), are shown in Extended Data Fig. 2.

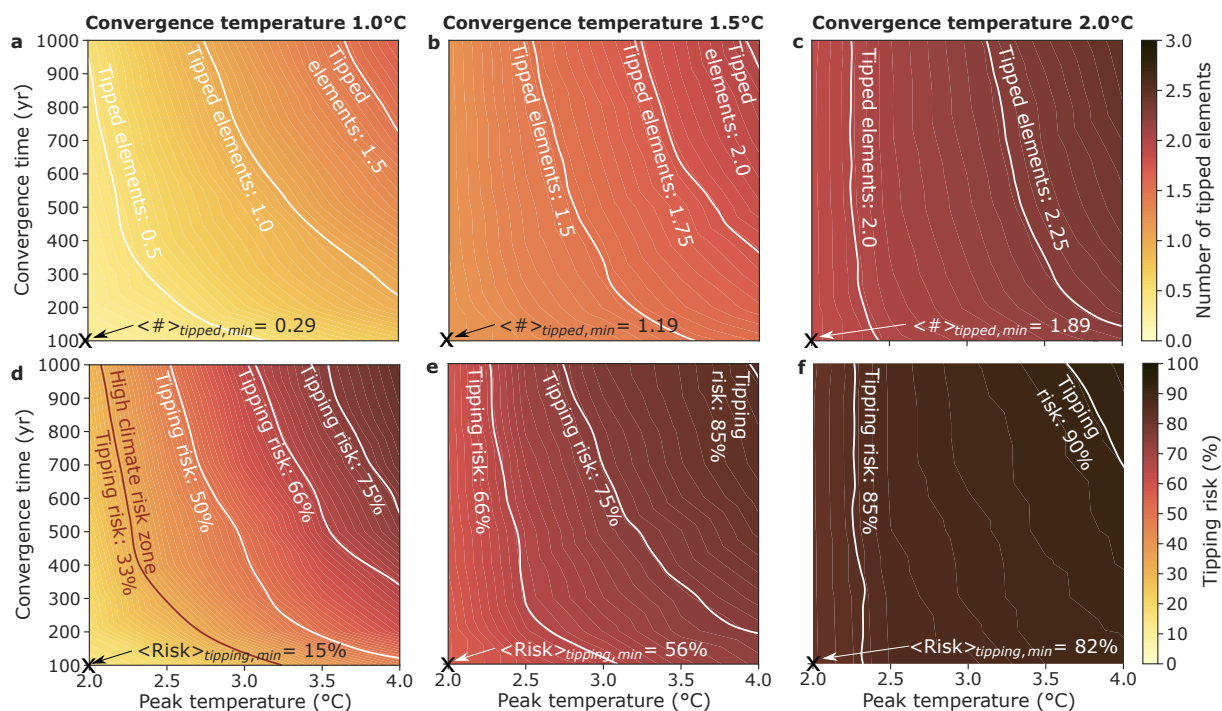


Fig. 3 | Expected number and risk of tipping events at different convergence temperatures.

a, Number of tipped elements averaged over the entire ensemble for all investigated convergence times t_{Conv} and peak temperatures T_{Peak} at a convergence temperature of $T_{\text{Conv}} = 1.0^\circ\text{C}$ above pre-industrial levels. The white lines show the conditions at which 0.5, 1.0, and 1.5 elements are tipped on average. $\langle \# \rangle_{\text{tipped}, \text{min}}$ is the average number of tipped elements at $t_{\text{Conv}} = 100$ years and $T_{\text{Peak}} = 2.0^\circ\text{C}$. **b**, **c**, Same as in **a**, but for convergence temperatures of 1.5°C and 2.0°C , respectively. **d**, The risk that at least one tipping element transitions to its alternative state in equilibrium (after 50,000 simulation years) for a convergence temperature of 1.0°C . The equipotential line in red indicates the *high climate risk zone* (tipping risk is equal to 33%). $\langle \text{Risk} \rangle_{\text{tipping}, \text{min}}$ is the average risk of at least one element being tipped at $t_{\text{Conv}} = 100$ years and $T_{\text{Peak}} = 2.0^\circ\text{C}$. **e**, **f**, Same as for **d**, but for convergence temperatures of 1.5°C and 2.0°C , respectively. The simulations for $T_{\text{Conv}} = 0.0^\circ\text{C}$ (return to pre-industrial temperatures) and $T_{\text{Conv}} = 0.5^\circ\text{C}$ can be found in Extended Data Fig. 4. High-end scenarios with $T_{\text{Peak}} = 4.0\text{--}6.0^\circ\text{C}$ are added in Extended Data Figs. 5, 6.

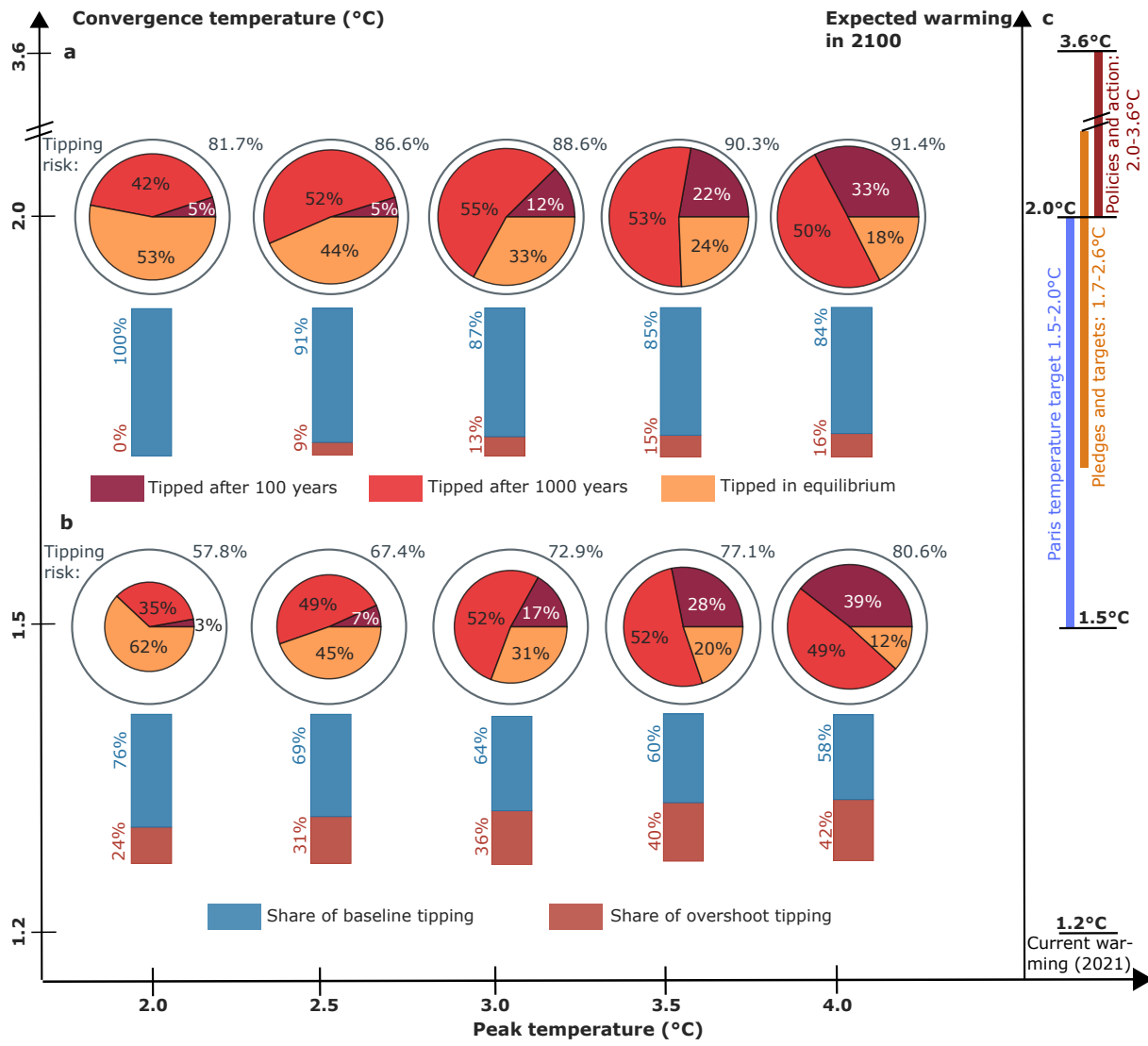
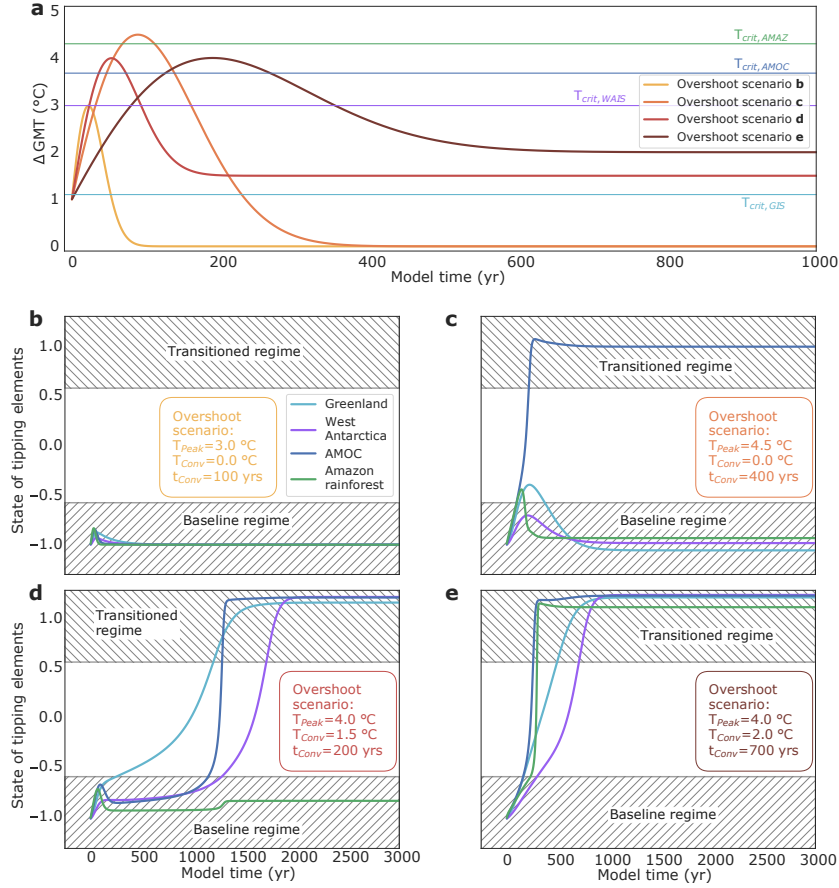
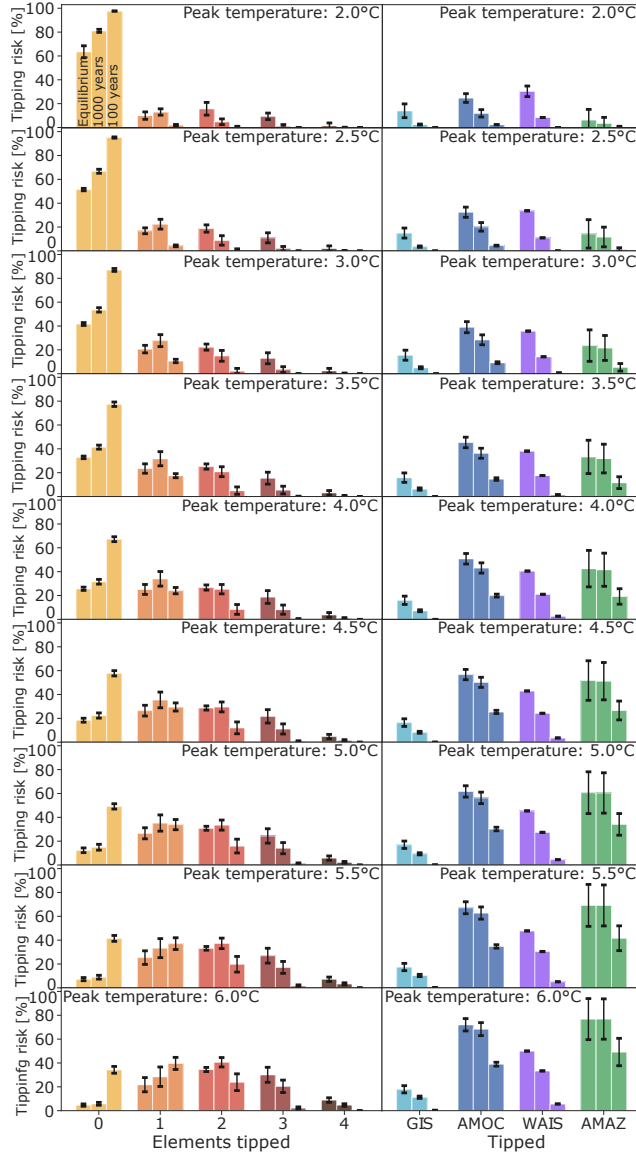


Fig. 4 | Timing and mechanisms of tipping events following temperature overshoots. Tipping risk with respect to overshoot scenarios of 2.0–4.0°C and convergence temperatures within the Paris range of 1.5–2.0°C above pre-industrial levels. The *pie charts* split the tipping events into the time-scale when they occur. Either after 100 simulation years (dark red), 1,000 simulation years (light red), or in equilibrium simulations (after 50,000 simulation years, orange). The size of the pie chart indicates the overall tipping risk (e.g. 67.4% at $T_{\text{Conv}}=1.5^\circ\text{C}$ and $T_{\text{Peak}}=2.5^\circ\text{C}$). The *bar chart* directly below the pie chart indicates the ratio between the two possible tipping mechanisms: (i) due to the convergence temperature being above the critical temperature for one or several tipping elements (*baseline tipping*, example see Greenland Ice Sheet in Extended Data Fig. 1d, e), and (ii) due to the overshoot trajectory (*overshoot tipping*, example see AMOC in Extended Data Fig. 1c). **a**, Scenario where global mean temperature converges to 1.5°C, or **b**, to 2.0°C. **c**, Expected warming in 2100 after the COP26 *pledges and targets* (orange vertical line: 1.7–2.6°C), and the *policies and action* (dark red vertical line: 2.0–3.6°C) together with the current warming of 1.2°C and the Paris temperature target (blue vertical line: 1.5–2.0°C). Note that the vertical axes are nonlinear due to visibility. The data for the vertical lines has been compiled from the November 2021 update by climateactiontracker¹⁴. The scenarios with lower convergence temperatures of 0.0, 0.5, and 1.0°C above pre-industrial are depicted in Extended Data Fig. 7. High-end climate scenarios and overshoots for peak temperatures between 4.5–6.0°C are shown in Extended Data Fig. 8.

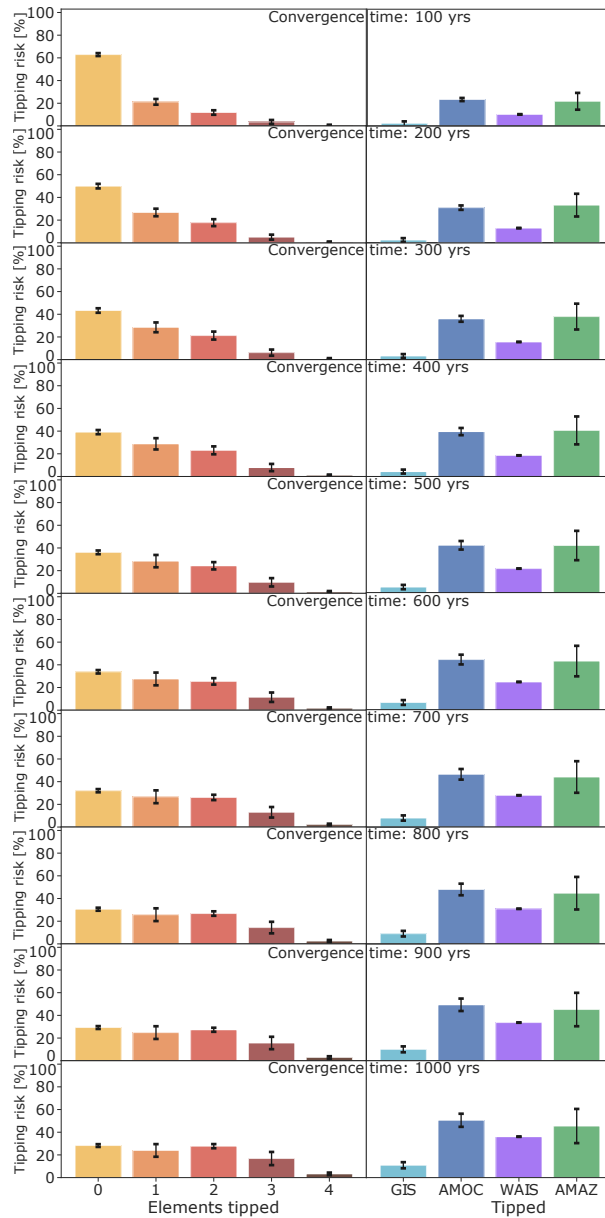
600 **Extended Data Figure legends.**



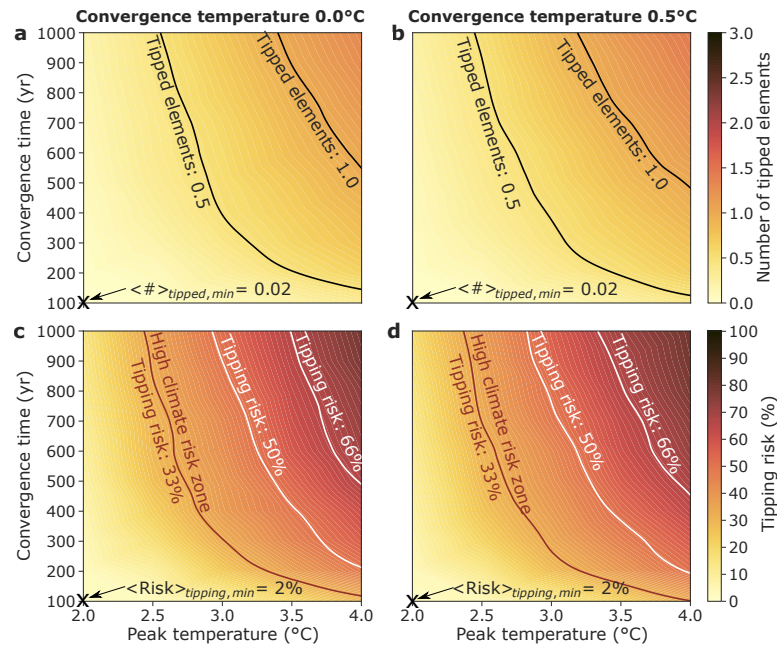
Extended Data Fig. 1 | Exemplary overshoot trajectories and their impact on tipping events. **a**, Time series of four different exemplary overshoot trajectories in dependence of the global mean surface temperature increase above pre-industrial levels (ΔGMT). Additionally, the four horizontal coloured lines show the critical temperatures of the Greenland Ice Sheet (GIS), the West Antarctic Ice Sheet (WAIS), the AMOC and the Amazon rainforest (AMAZ) for this specific ensemble member (for the entire ensemble of overshoots and tipping element set-ups, see Methods). **b–d**, The impact on tipping events in response to the applied overshoot scenario. Even though we only show one exemplary ensemble member here, it is apparent that higher temperature stabilisation levels (T_{Conv}) lead to a higher number of tipped elements (compare scenarios in **b**, **c** with scenarios in **d**, **e**), but also higher peak temperatures and convergence times have the same effect. The parameter values for this example are (same as in Fig. 1a,b): $T_{\text{crit, GIS}} = 1.1^\circ\text{C}$, $T_{\text{crit, AMOC}} = 3.6^\circ\text{C}$, $T_{\text{crit, WAIS}} = 3.0^\circ\text{C}$, $T_{\text{crit, AMAZ}} = 4.3^\circ\text{C}$, $s_{\text{GIS}\rightarrow\text{WAIS}} = 9.2$, $s_{\text{AMOC}\rightarrow\text{GIS}} = -3.1$, $s_{\text{GIS}\rightarrow\text{AMOC}} = 9.5$, $s_{\text{WAIS}\rightarrow\text{AMOC}} = 1.1$, $s_{\text{WAIS}\rightarrow\text{GIS}} = 1.5$, $s_{\text{GIS}\rightarrow\text{WAIS}} = 1.5$, $s_{\text{AMOC}\rightarrow\text{AMAZ}} = 3.0$, $\tau_{\text{GIS}} = 1602$ yrs, $\tau_{\text{AMOC}} = 172$ yrs, $\tau_{\text{WAIS}} = 1008$ yrs and $\tau_{\text{AMAZ}} = 56$ yrs. The interaction strength parameter is set to $d = 0.20$. For more details on the parameter values and meaning, see Methods.



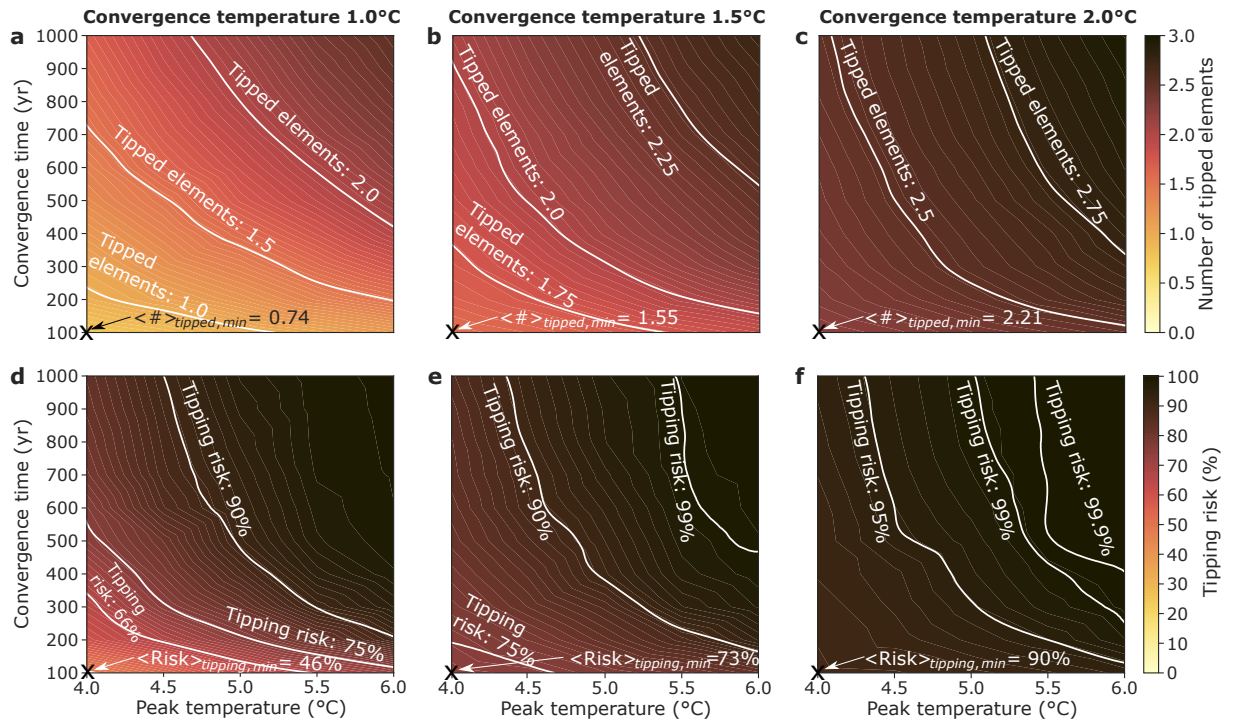
Extended Data Fig. 2 | The effect of time scales in overshoot scenarios on the risk for tipping events. In the left column, the probability of zero, one, two, three, or four tipped elements are shown for peak temperatures between $T_{\text{Peak}} = 2.0^\circ\text{C}$ (lowest scenario) up to $T_{\text{Peak}} = 6.0^\circ\text{C}$ (highest scenario). The right column breaks down the respective elements, which are responsible for the respective average number of tipped elements from the left column. The three parallel drawn bars in each panel detail the time scale of tipping into three scenarios. The left bar shows the result in equilibrium simulations (after 50,000 simulation years, long-term tipping), the bar in the middle shows the tipping events after 1,000 simulation years (mid-term tipping), and the right bar after 100 simulation years (short-term tipping). We depict the average over the entire ensemble as the bar height and the error bars show the standard deviation.



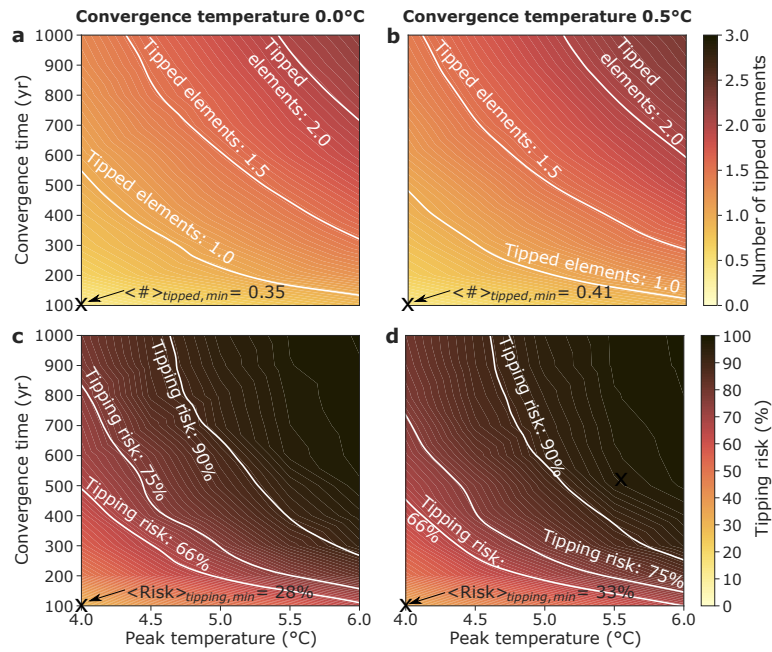
Extended Data Fig. 3 | The effect of the convergence time on the risk for tipping events. In the left column, the probability of zero, one, two, three, or four tipped elements are shown for convergence times of $t_{\text{Conv}} = 100$ years (uppermost row) up to $t_{\text{Conv}} = 1,000$ years (lowermost row). The right column breaks down the respective elements, which are responsible for the respective average number of tipped elements from the left column. We depict the average of the equilibrium run (long-term tipping after 50,000 simulation years) over the entire ensemble as the bar height and the error bars show the standard deviation.



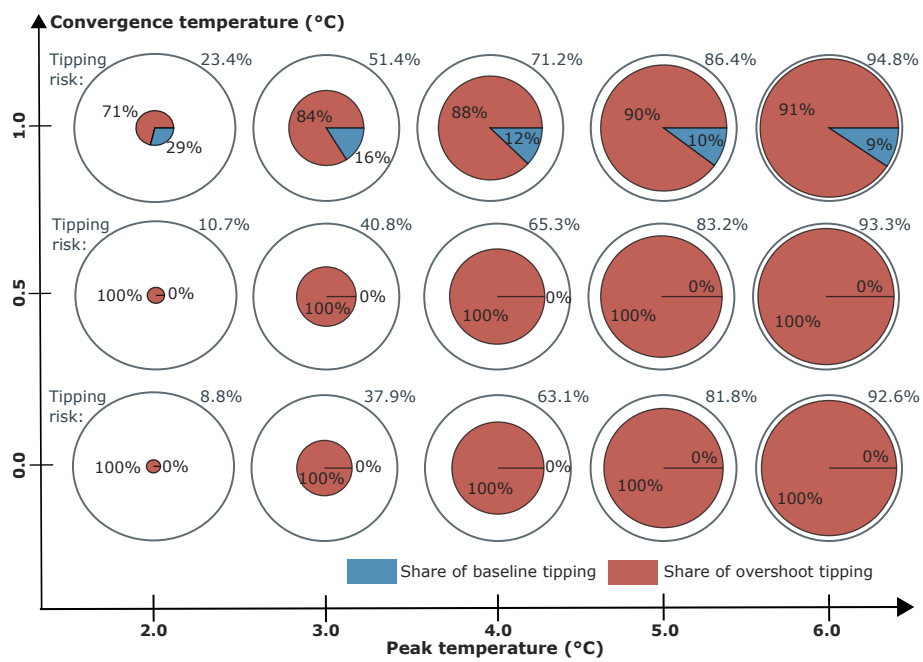
Extended Data Fig. 4 | Expected number and risk of tipping events at low convergence temperatures. Same as in Fig. 3 in the main manuscript, where the average number of tipped elements is shown for a set of convergence times and peak temperatures at a convergence temperature of **a**, 0.0°C (return to pre-industrial levels) and **b**, 0.5°C. The respective tipping risk that at least one tipping element ends up in the tipped regime is shown in panels **c**, **d**. Note that the *high climate risk zone* commences at higher peak and convergence times as compared to Fig. 3d in the main manuscript.



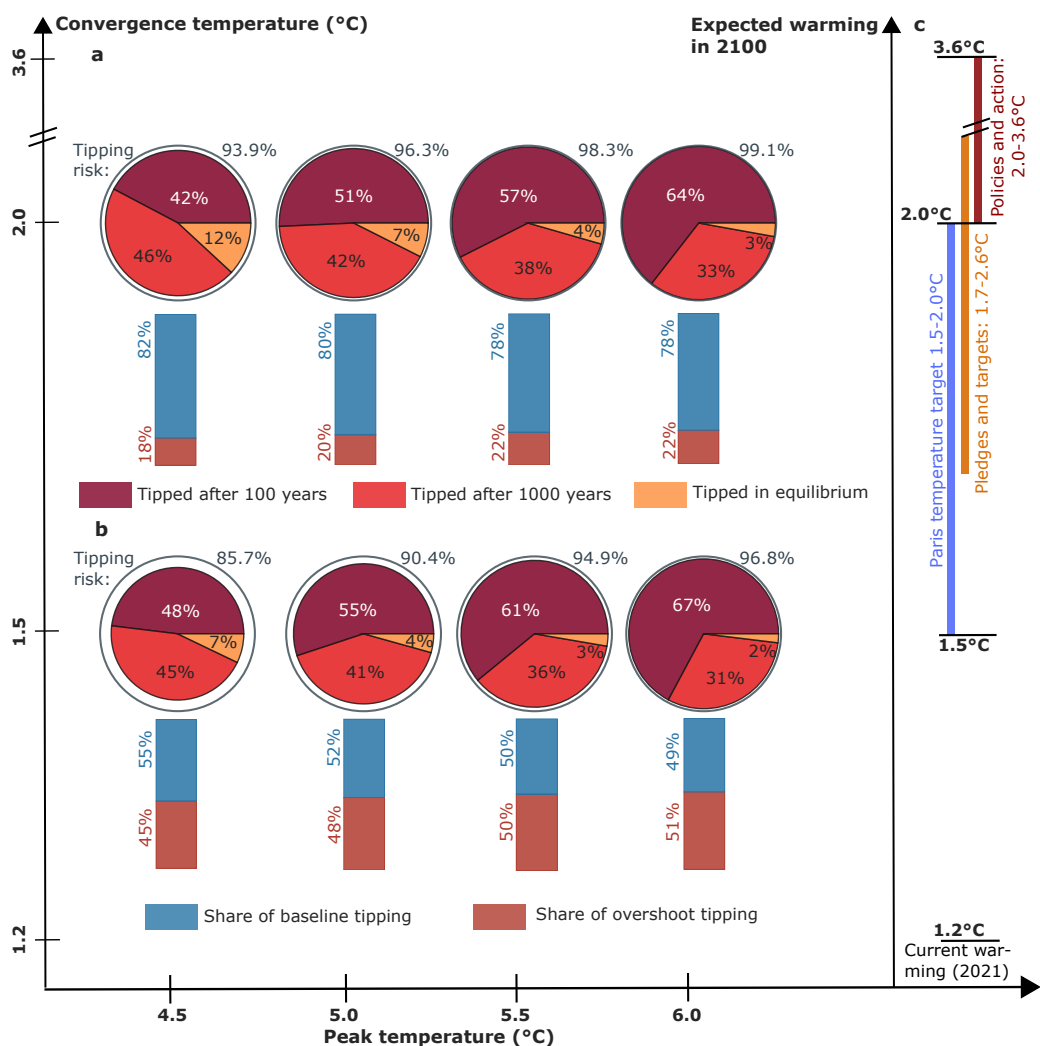
Extended Data Fig. 5 | Expected number and risk of tipping events for high-end temperature overshoots. Same as in Fig. 3 in the main manuscript, where the average number of tipped elements is shown for a set of convergence times and peak temperatures at a convergence temperature of **a**, 1.0°C, **b**, 1.5°C, and **c**, 2.0°C. The respective tipping risk that at least one tipping element ends up in the tipped regime is shown in panels **d**, **e**, **f**. For all high-end scenarios, the tipping risk for one tipping event to occur $\geq 75\%$ if final convergence temperatures are between 1.5–2.0°C above pre-industrial levels.



Extended Data Fig. 6 | Expected number and risk of tipping events for high-end temperature overshoots at low convergence temperatures. Same as in Extended Data Fig. 3, where the average number of tipped elements is shown for a set of convergence times and peak temperatures at a convergence temperature of **a**, 0.0°C (return to pre-industrial levels) and **b**, 0.5°C. The respective tipping risk that at least one tipping element ends up in the tipped regime is shown in panels **c**, **d**.



Extended Data Fig. 7 | Mechanism for tipping following a temperature overshoot for low T_{Conv} . Same as Fig. 4 of the main manuscript, but for lower convergence temperatures of 0.0, 0.5 and 1.0°C. To depict the tipping risk visually as the size of the pie charts, the reason (baseline or overshoot tipping) for tipping is depicted in the respective pie charts.



Extended Data Fig. 8 | Mechanism and timing of tipping events following a high-end temperature overshoot. Same as in Fig. 4 of the main manuscript, but for higher temperature overshoot trajectories peaking between 4.5–6.0°C. In these cases, tipping also plays a very important role at shorter timescale of 100 years, see the increasing fraction of the dark red part in the pie charts. **a**, Convergence temperature of 1.5°C, **b**, Convergence temperature of 2.0°C.